ISSN: 2634 - 8853

Journal of Engineering and Applied Sciences Technology

SCIENTIFIC Research and Community

Research Article

Open Access

Evaluation of CO2 Injection in Shale Gas Reservoirs Based on Numerical Simulation

Steve Wilfried Nzuetom Mbami

China University of Petroleum (East China), China

ABSTRACT

Shale gas is natural gas that is found trapped within a typical sedimentary rock derived from clastic sources which is known as shale. The combination of two advanced technologies (horizontal drilling and hydraulic fracturing) has helped to access to a large volumes of shale gas that was previously not producible. In this paper, the performance of CO2 injection and CH_4 recovery in shale gas reservoirs is evaluated. The study reveals that it is a complex function a several parameters such as CO2 injection time, soaking time, injection volume, reservoir permeability, reservoir porosity, and thickness. Numerical simulation is performed to model CO2 huff-n-puff process and multicomponent Langmuir isotherms in the Barnett Shale formation; two horizontal wells are performed for this case. Results show that CO2-EGR is very efficient for shale gas and a recovery factor of 82.6% can be obtained by this process. Besides, an analytical study is done in order to facilitate the estimation of recovery factor based on critical parameters obtained from simulation. A comparison study of the observed data from simulation and the estimated date from some production decline models such as LGA (Logistic Growth Analysis) model, and Ali model is also performed in this study.

***Corresponding author**

Steve Wilfried Nzuetom Mbami, China University of Petroleum (East China), China. E-mail: nzuetomsteve@yahoo.com

Received: August 19, 2021; **Accepted:** August 31, 2021; **Published:** September 05, 2021

Keywords: Shale Gas Reservoirs, Numerical Simulation, CO2 Huff-N-Puff, Enhanced Gas Recovery, Production Decline Model

Introduction

The demand for unconventional energy, and the exploration and development of unconventional resources such as shale gas formation has gradually increased due to the rapid consumption of conventional energy [1]. Shales have these particularities that they are characterized by an extremely small grain size, low permeability and porosity, and high total organic carbon (TOC). According to Kang et al., the organic matter is a material with ultra-low porosity that consists of micropores and mesopores [2]. Natural gas in shale formation can be stored as free gas in mineral pore and organic matter [3]. Two forms for natural gas flow through shale matrix to fractures usually happen depending on the matrix being organic or inorganic. In organic matrix pores, the dominance is materialized by the transition diffusion mechanism and the effect produced by slip; however, gas-water two-phase flow controls the gas transport in inorganic matrix pores [4]. Under isothermal conditions in shale gas reservoirs (the development process is considered to be an isothermal process), there are several mechanisms for gas mass transport: viscous flow, Knudsen diffusion, adsorption/desorption effects, surface diffusion [5]. Bird et al. has discovered that the different transport mechanisms of gas in shale gas reservoirs interacted with each other, making the gas migration mode more complicated. At the same time, the special gas storage structure of reservoirs has increased the difficulty of numerical simulation rock gas reservoirs. CO2 has been chosen here as the ideal solvent in order to enhance the gas recovery. It has been proved that shale gas has a stronger affinity to CO2 thanCH_4 (Kang SM et al., 2011; Ambrose RJ et al., 2012) which means the gas shale will absorb more CO2 when they exist at the same time [2,6,7]. Shale and CO2 affinity is partly of steric and thermodynamic effects, which is same with the consideration of coal for enhanced coalbed methane (ECBM) recovery [2]. One of the important mechanism of CO2 injection is that the adsorption capacity of shale for CO2 is larger than that for methane and some studies show that CO2 is preferentially adsorbed over CH_4 with a ratio up to 5:1. Thus, CO2 could replace the absorbed methane via competitive adsorption when CO2 is introduced in shale [1,8-10].

Fathi and Akkutlu have concluded that enhanced methane recovery is divided into three stages [11]: (1) consecutive/dispersive flow gas phase (injected CO2 released CH_4 molecules), particularly in fractures; (2) diffusive/dispersive gas transport in the secondary pore shale matrix, ie., fractures and macro-pores; and (3) multi-component sorption phenomena, particularly in primary (micro) pore structure of the shale matrix, eg., co- and counter diffusion and competitive adsorption. The effect of hydraulic fractures illustrated by Kalantari D and multi-component transport and stress change during CO2 injection have also been conducted [12,13]. In the recent years, two special types of production modes have been done among the CO2 injection into shale gas reservoir works: CO2 flooding and CO2 huff-n-puff. In CO2 flooding, one well is used injection while the other well produces all the time. In CO2 huff-n-puff, a well goes through three stages: injection, soaking time and production [14]. Kim et al. evaluated CO2 injection using different shale models considering multi-component adsorption and stress-dependent permeability [13]. It is observed that both CO2 flooding and CO2 huff-n-puff can increase the gas recovery, though CO2

huff-n-puff is not preferred compared to the flooding case. Also, more CO2 can be stored underground when us CO2 flooding. Liu et al. presented a novel methodology based on nuclear magnetic resonance (NMR) [15]. It can be used to measure the enhanced gas recovery (EGR) efficiency caused by CO2 injection. Sun et al. have proved that CO2 sequestration with enhanced natural gas recovery can achieve CO2 sequestration and CH_4 recovery in shale gas reservoirs, and the injection pressure has a huge impact on CO2 storage and natural gas production rate [16].

Many studies have proved that the Barnett shale formation has a high potentiality of natural gas; it has been a source of interest for many researchers. Barnett shale is located in the Fort Worth Basin of northern Texas, and its potential natural gas production was discovered in 1981 by Mitchell Energy [17]. Vermylen after performing N_2, CO2 and CH_4 adsorption isotherms test on four Barnett shale samples, has found that and found that CH_4 and N_2 showed Langmuir adsorption type, while three samples demonstrated Brunauer-Emmett-Teller (BET) adsorption type for CO2 and one sample demonstrated Langmuir adsorption type for CO2. In this work, Barnett shale data is used for history matching [18]. Based on that data, we created a numerical simulation model. CMG-GEM is used here as the appropriate simulator in other to reach our goals. CO2 huff-n-puff injection in two horizontal wells is performed for sensitivity studies. Four uncertain parameters (CO2 injection time, soaking time, reservoir permeability and reservoir porosity) are revealed.

Mathematical Model for CO2 Injection in Shale Gas Reservoirs

Some assumptions are made when establishing our model: gas is stored in natural and primary fractures as free gas; in the matrix it is stored as both free and adsorbed phase. The general equations of various interactions between continuums are:

$$\frac{\partial}{\partial t}\left\{\phi\rho_g x_i + (1-\phi)m_i\right\} = \nabla.\left(\rho_g x_i \upsilon\right) + q_i^w + q_i^{conn} \quad (1)$$

Introducing Darcy's law:

$$\upsilon = \frac{k}{\mu}\left(\nabla p - \gamma g \nabla D\right) \quad (2)$$

The formula of the mole of component i adsorbed in unit formation volume, (only for matrix):

$$m_i = \rho_R \rho_{gs} V_i \quad (3)$$

Where ϕ is the porosity of the matrix or fractured media; k is the apparent permeability of matrix or pressure-dependent permeability of fractures; μ is the gas viscosity; γ is the mass density of gas mixture; ρ_g is the gas molar density; x_i is the component mole fraction; ρ_R is the rock bulk density; ρ_{gs} is the gas molar density at standard condition; V_i is the adsorption isotherm function; q^w_i is the source/sink term of component i; q_i^{conn} is the flux terms of component i between continuums.

Physical Properties of CH_4 and CO2

A good knowledge of thermodynamic properties of Methane (CH_4 and carbon dioxide (CO2) is important to achieve our goal thus they have a great responsibility on monitoring transportation, optimizing compression and modeling mobility of gas in the reservoir conditions. Table 1 listed some key parameters of methane and carbon dioxide. Thus, it is important to notice that CO2 behaves as a supercritical fluid which has viscosity of a gas and density of a liquid at deep reservoir conditions. The higher density reveals that CO2 will migrate downward in the reservoir as relative to CH_4. The analysis of Chapela and Rowlinson equation deduces CO2 density. Similarly,CH_4 density is obtained by using Jacobsen and Stewart equation [19,20]. It can be seen that CO2 is highly denser than CH_4 throughout the reservoir pressure range. Chang et al. results have shown that by using their correlations, the CO2 solubility can be modeled. Similarly, Duan and Mao study reveals that CH_4 solubility in aqueous phase can be modeled by their correlations. There are fewer tendencies to finger and intermix between the gases due to these properties [21-23].

Table 1: Matched values for reservoir and geomechanical properties from history matching

Properties	Values
Initial Reservoir Pressure	3800 psi
Porosity	0.06
Matrix permeability	0.0004 md
Reservoir Temperature	140 °F
Young's Modulus	3,887,500 psi
Poison's Ratio	0.2095
Natural Fracture Permeability	0.007 md

Adsorption of CO2 and CH_4 in Barnett Shale

Previous studies have proved that the adsorption at the gas/solid interface is related to the enrichment of one or more components in the interfacial layer. Previous studies have proved that the adsorbed gas has a higher density than the surrounding non-adsorbed gas. According to Clarkson and Haghshenas there are five mechanisms for methane existence in shale gas reservoirs: Adsorption upon internal surface area, conventional (compressed gas) storage in natural and hydraulic (induced) fractures, conventional storage in matrix porosity (organic and inorganic), solution in formation water, and absorption (solution) in organic matter. According to the International Union of Pure and Applied Chemistry (IUPAC) standard classification system there are six different types of adsorption, as in Figure 1. The classic Langmuir isotherm (Type I) is considered as the most commonly applied monolayer adsorption model for shale gas reservoirs. It is based upon the assumption that there is a dynamic equilibrium at constant temperature and pressure between adsorbed and non-adsorbed gas [24-26]. The following formula described the Langmuir isotherm with two fitting parameters:

$$V(P) = \frac{V_L P}{P + P_L} \quad (4)$$

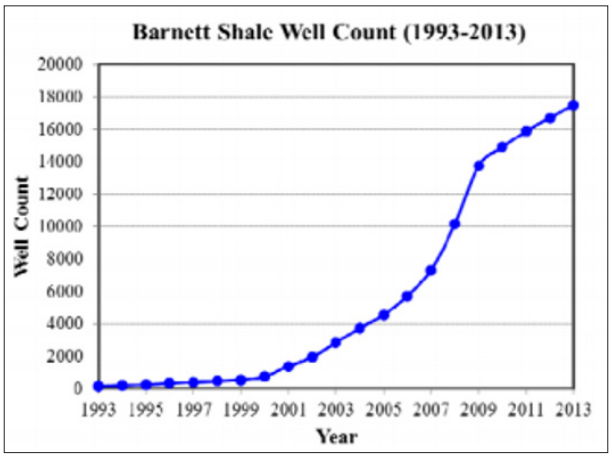

Figure 1: Barnett Shale well count. Source: Texas Railroad Commission (modified from Texas Railroad Commission, 2013)

Where $V(P)$ is the gas volume of adsorption at pressure P, V_L is Langmuir volume, referred to as the maximum gas volume of adsorption at the infinite pressure, P_L is Langmuir pressure, which is the pressure corresponding to one-half Langmuir volume. According to Gao et al. the instantaneous equilibrium is a reasonable assumption because ultra-low permeability in shale leads to very low flow rate through the kerogenic media within shale. It is also assumed to be established for the Langmuir isotherm. In the case of multilayer sorption of gas occurs, the BET isotherm (Type II) should be a better model the following equation materialize that fact [27-29]:

$$V(P) = \frac{V_m CP}{(P_o - P)\left[1 + (C-1)P/P_o\right]} \quad (5)$$

Where P_o is the saturation pressure of the gas, V_m is the maximum adsorption gas volume when the entire adsorbent surface being covered with a complete unimolecular layer, C is a constant related to the net heat of adsorption. Figure 2 describes other isotherm types [24].

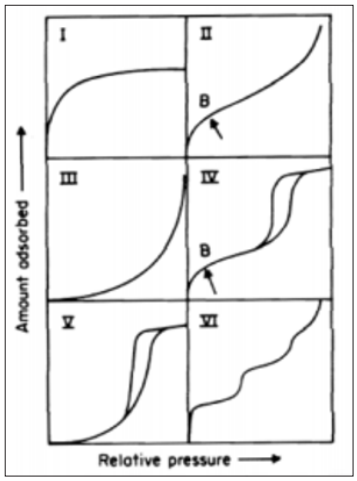

Figure 2: The six types of Physisorption isotherms according to the IUPAC classification (Sing et al., 1985).

Numerical Simulation Model

In this work, CMG-GEM simulator is used to model CO2 flow in a shale gas reservoir. Arri et al, 1992; Hall et al., 1994 through GEM simulator used an extended Langmuir isotherm for modeling multicomponent adsorption and desorption. The following formula is best explicit [30,31]:

$$w_i = \frac{w_{i\max} B_i y_{ig} p}{1 + p\sum_j B_j y_{jg}} \quad (6)$$

Where w_i is the moles of adsorbed component i per unit mass or rock, wi_{max} is the maximum moles of adsorbed component i per unit or rock, B_i is the parameter for Langmuir isotherm relation, p is pressure, and y_ig is the molar fraction of adsorbed component i in the gas phase, i and j are component indices including CH_4, N_2, CO2, or coal. To evaluate the effects of CO2 injection in shale gas reservoir, a 3D shale reservoir model of 30 ft × 20 ft × 10 ft Grid cells dimension in Figure 3 was built based on the properties of history matching. History matching was performing by using the field data of Barnett shale reproduced from Anderson et al. the matched values, segment of the rese, and other properties are shown in Table 1. The average matrix permeability of the reservoir is 24 mD and average porosity 0.4%. The average thickness of the reservoir is 5ft and the reservoir temperature is a constant 140 °F. Figure 4 shows the average reservoir pressure during the whole life of the reservoir [32].

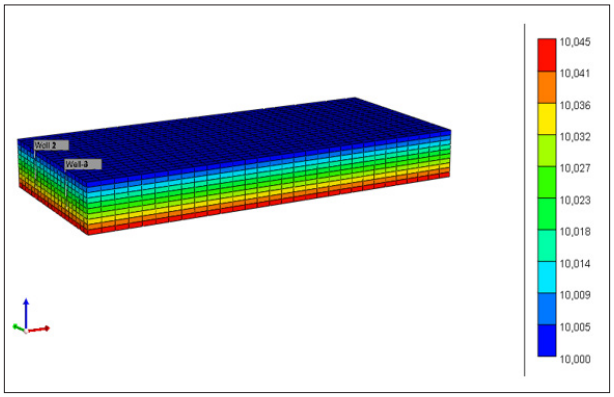

Figure 3: 3D reservoir model including 2 horizontal wells

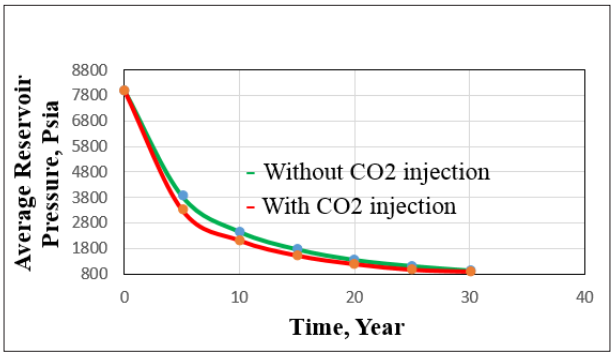

Figure 4: Average reservoir pressure with and without CO2 injection

Results and Discussion

Two horizontal wells were performed in this work. Based on our previous researches, we chose CO2 huff-n-puff process in other to minimize spending. This process is applying to the two wells at the same time. For our base case, we injected CO2 for 6 months; after that we shut-in the wells for a period of time (soaking time) of 3 months and finally wells started producing for 24 months. The cycle is repeating until the end of the production period of 30 years. Figure 5 and Figure 6 indicate respectively the gas recovery and the cumulative gas production with and without CO2 injection. We can notice that the recovery factor of the gas is lower without CO2 injection, thus it is useful for the displacement of the methane. The adsorbed moles of CH_4 and CO2 without considering multi-component adsorption mechanism is presented in Figure 7. The figure shows that the potential adsorption of CH_4 decreases with the production time while there is not CO2 adsorption. Figure 8 shows the total volume of CO2 injected in the reservoir. It can be seen that a total amount of 350 Mscf of CO2 is injected.

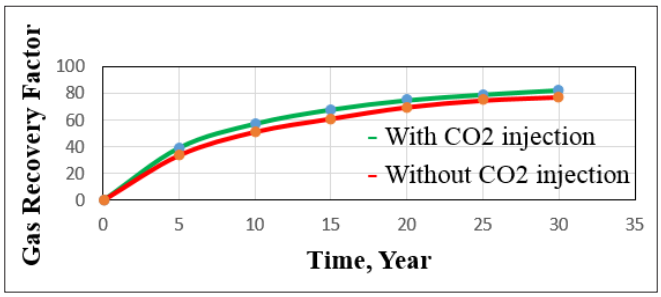

Figure 5: Comparison of gas recovery factor with and without CO2 injection

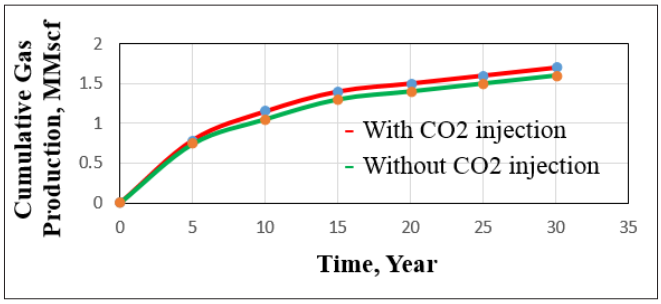

Figure 6: Cumulative gas production with and without CO2 injection

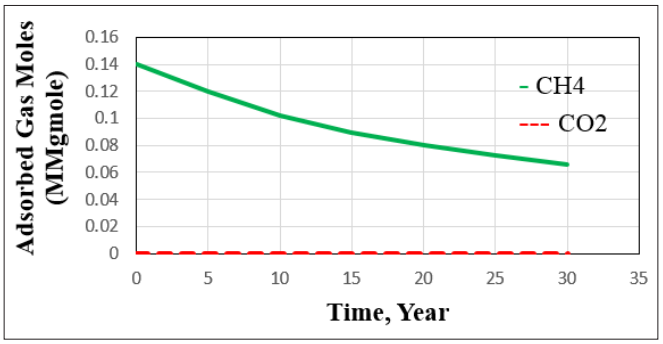

Figure 7: Adsorbed gas moles for CO2 and CH4 without considering multi-component adsorption

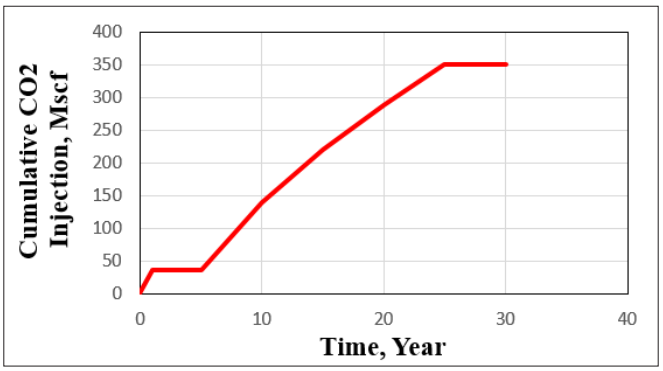

Figure 8: Total volume of CO2 injected

A sensitivity study was done in other to analyze all the parameters that can affect the methane recovery. Due to many estimable and uncertain parameters such as reservoir permeability, porosity, fracture half-length, and fracture conductivity there is a high uncertainty in shale gas reservoirs 33-35. The present work considered four uncertain parameters such as reservoir permeability, porosity, CO2 injection time, and number of cycle (as listed in Table 2) for maximizing the methane recovery. Figure 9 shows that the increase of the reservoir permeability increases the methane recovery. This is because the increase of permeability affects directly the mobility ratio then affects the gas recovery. The maximum value of gas recovery factor obtained is 89.4 %. The effect of the reservoir porosity on the methane recovery is shown in Figure 10. We can understand that the increase of reservoir porosity increases the gas recovery. The maximum value of gas recovery obtained is 86.4%. Figure 11 and Figure 12 respectively analyze the effect of CO2 injection time and the number of cycle on gas recovery. It can be seen that they increase the methane recovery in a certain condition. The maximum values of gas recovery obtained are respectively 83.3% and 82.6%.

Table 2: Four uncertain parameters used for sensitivity study

Parameter	Value 2	Base Case	Value 3
Reservoir Permeability	0.0008	0.0004	0.009
Reservoir Porosity	0.03	0.06	0.09
CO2 Injection Time	3	6	9
Number of Cycle	3	11	7

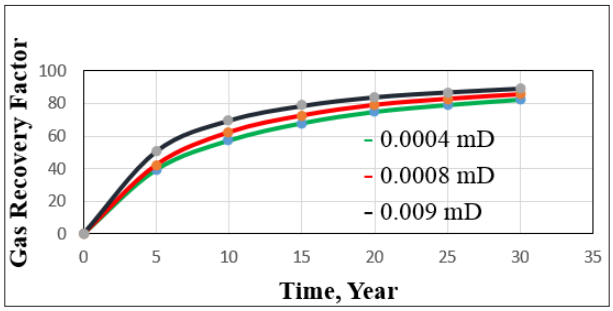

Figure 9: Effect of Reservoir permeability on gas recovery factor

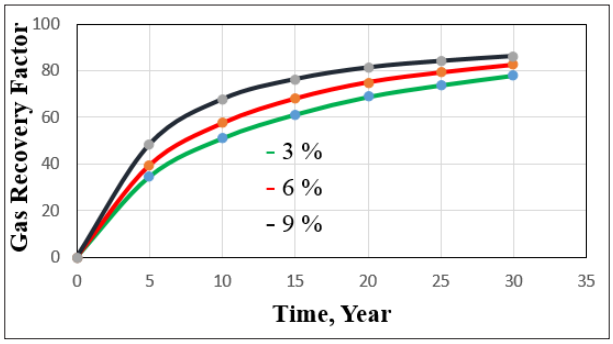

Figure 10: Effect of Reservoir porosity on gas recovery factor

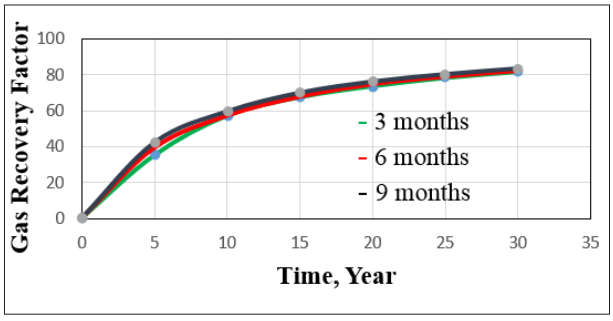

Figure 11: Effect of CO2 injection time on gas recovery factor

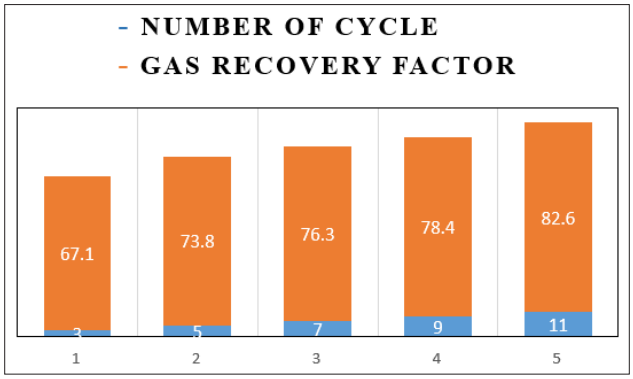

Figure 12: Effect of number of cycle on gas recovery factor

Besides, some regression equations were built for analytical solutions. These equations are obtained based on simulation results. They can be used to get an approximatively value of the gas recovery factor just by replacing the unknown X by the value of one of the uncertain parameters listed above. Figure 13, Figure 14 and Figure 15 respectively illustrate the gas recovery in function of reservoir permeability, number of cycle, and CO2 injection time.

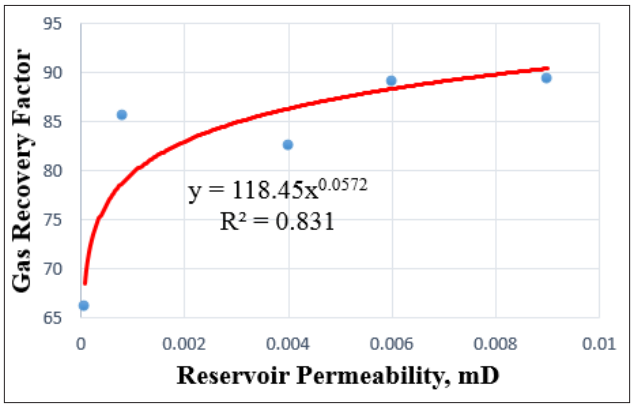

Figure 13: Gas recovery factor versus reservoir permeability

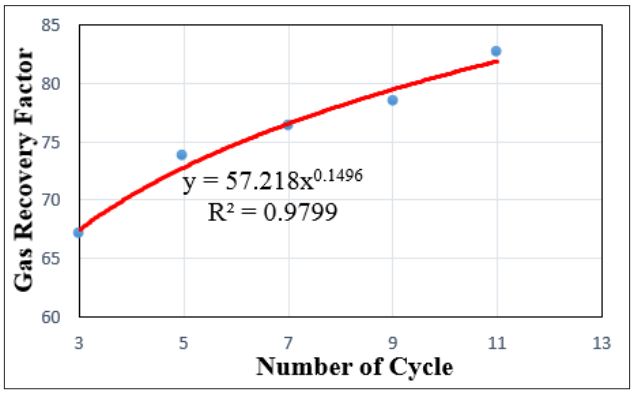

Figure 14: Gas recovery factor versus number of cycle

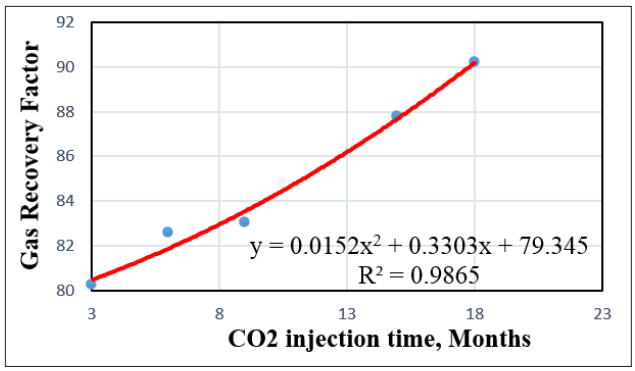

Figure 15: Gas recovery factor versus CO2 injection time

Finally, a comparison study observed data (from simulation results) and estimated data (from production decline models) was performed. Two production decline models have been chosen for our work: Logistic Growth Analysis (LGA) model and Ali model. Clark et al. by matching the logistic growth model to the production data of some wells have built an update time-rate function [36]. LGA model is proposed for estimating production forecasting of reservoirs with extremely low permeability [36,37]. The following equation has been derived from the hyperbolic group of curves and is usually used for the cumulative production estimation;

$$Q(t) = \frac{Kt^n}{a + t^n} \qquad (7)$$

where K is the carrying capacity or the maximum recoverable gas from the reservoir. 'a' constant is t^n at which half of the recoverable gas has been produced. 'n' is the hyperbolic exponent.

In our study, the parameters K, a and n were estimated using Excel's multivariable solver tool. Comparison of the observed cumulative production with the one obtained by using Eq.7 has been done. The model has the same trend as the observed data but diverges from time to time as shown in Figure 16.

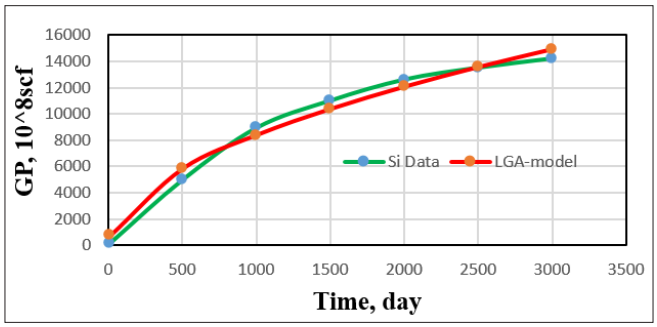

Figure 16: LGA model fit to cumulative gas production

Ali et al. have found that the plot of the cumulative gas production in function of time is a straight line with the slope equal to 1 if the flowing pressure of the production well is constant. However, many analyses have proved that the best relationship between both variables is:

$$G_p = ct^n \qquad (8)$$

Where c is the intercept constant and n (=dt^{-p}) is the slope parameter which is a time function defined as a power law function. The first step is to fit Eq.8 into the observed cumulative gas production to

estimate constant (c) using linear regression. Figure 17 shows the corresponding best fit parameter for the intercept c = 28.661 1/d. The next step is to estimate the change of slope (n) with time. The change of slope (n) can be calculated by inverting Eq.8 for each time step as n(slope) = (log(G_{p2})-log(G_{p1}))/ (log(t_2)-log(t_1)). Then we draw the slope points versus time on log-log plot. Figure 18 shows the change of slope over time, the best fit regression function is n = 1.554 $t^{-0.179}$. Comparison of the observed cumulative production with the one obtained by using Eq.8 has been done. The model's trend is the same with the observed data one. It matches the observed data at the beginning, then it starts diverging as shown in Figure 19.

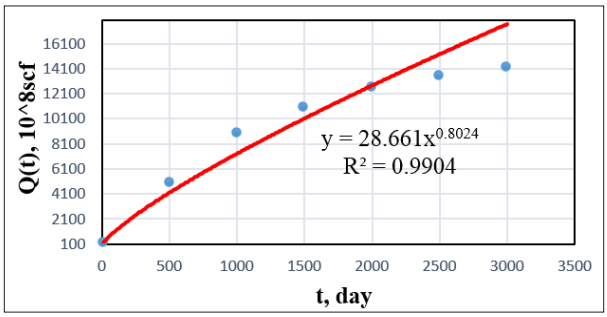

Figure 17: Cumulative gas production vs. actual time for Ali Model

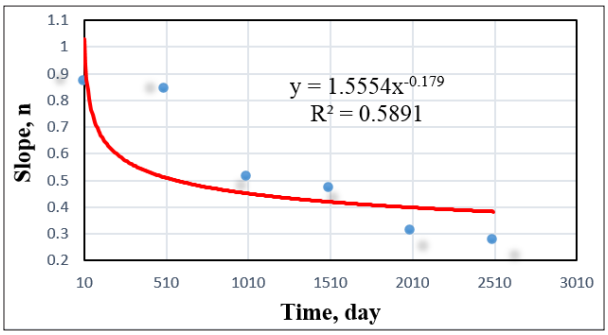

Figure 18: Slope (n) vs. actual time for Ali Model

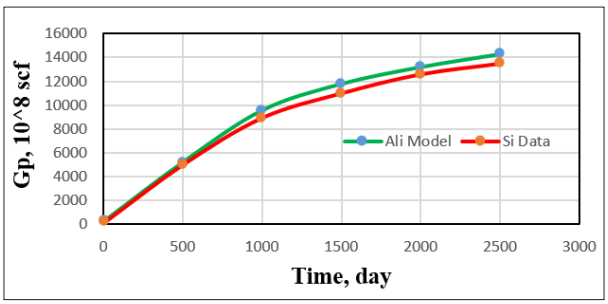

Figure 19: Ali model fit to cumulative gas production

Conclusion

In this study, a series of simulations have been done in other to evaluate the CO2-enhanced gas recovery in shale gas reservoirs. The following conclusions have been brought out:

1. Injection CO2 into shale gas reservoir can really enhance the gas recovery. Some parameters such as reservoir permeability, reservoir porosity, CO2 injection time and the number of cycle have a great effect on the methane recovery.
2. A comparison of the gas recovery factor with and without CO2 injection has illustrated that the effect is higher when CO2 is injected.
3. The physical properties of CO2 and CH_4 have proved that the range 3500-4700 ft is suitable for enhancing methane recovery and CO2 storage.
4. In the case of non-considering multicomponent adsorption there is not an adsorbed CO2 during the whole process.
5. LGA model and Ali model are two suitable models for estimating production forecasting of an unconventional reservoir.

Nomenclature

TOC = Total Organic Component

EGR = Enhanced Gas Recovery

LGA = Logistic Growth Analysis

ECBM = Enhanced Coalbed Methane

NMR = Nuclear Magnetic Resonance

BET = Brunauer Emmett Teller

IUPAC = International Union of Pure and Applied Chemistry

ϕ = Porosity

K = Permeability, md

ρ_g = Gas molar density,

x_i = Component mole fraction

m_i = Adsorbed mole in unit formation volume, kmol.ft^{-3}

q_i^w = Source/sink term, kmol. ft^{-3}

q_i^{com} = Flux term between continuums, kmol. $ft^{-3}.d^{-1}$

ι = Darcy velocity, ft^2.d^{-1}

γ = Gas mass density, ton. ft^{-3}

ρ_{gs} = Gas molar density at standard condition, kmol.ft^{-3}

V_i = Adsorption term, ft^{-3}. ton^{-1})

V_L = Langmuir volume, Scf/ton

P = Pressure, Psi

P_L = Langmuir pressure, Psi

V = Maximum adsorption gas volume, Scf/ton

C = Constant relate to the net heat adsorption

P_o = Saturation pressure of the gas, Psi

W_{imax} = Maximum moles of adsorbed component i per unit mass or rock, mole

B_i = Parameter for Langmuir isotherm relation

yig = Molar fraction of adsorbed component i in the gas phase

a = Intercept constant defined in LGA Model

k = Maximum recoverable gas from the reservoir

G_p = Cumulative gas production, Scf

C = Intercept constant defined in Ali Model

References

1. Pan JP (2012) Consideration of several issues in promoting shale gas exploration and development in China [J]. International Petroleum Economics Z1: 101-106.
2. Kang SM, Fathi E, Ambrose RJ, Akkutlu IY, Sigal RF (2011)

Carbon Dioxide Storage Capacity of Organic-rich Shales. SPE J 16: 842-855.

3. Leahy-Dios A, Das M, Agarwal A, Kaminsky R (2011) Modeling of Transport Phenomena and Multicomponent Sorption for Shale Gas and Coalbed Methane in an Unstructured Grid Simulator. Paper SPE 147352 SPE Annual Technical Conference and Exhibition Denver CO2
4. Shi J, Zhang L, Li Y, Yu W, He X, et al. (2013) Diffusion and Flow Mechanisms of Shale Gas through Matrix Pores and Gas Production Forecasting. Paper SPE 167226 SPE Unconventional Resources Conference 5-7.
5. Clifford K Ho, and Webb SW (2006) Gas Transport in Porous Media [M]. Netherlands: Springer.
6. Bird RB, Stewart E, Lightfoot EN (2002) Transport phenomena [M]. New York USA: John Wiley & Sons Inc.
7. Ambrose RJ, Hartman RC, Diaz-Campos M, Akkutlu IY, Sondergeld CH (2012) shale gas in place calculations part I: new pore-scale considerations. SPE J 17: 219-229.
8. Yuan W, Pan Z, Li X, Yang Y, Zhao C, et al. (2014) Experimental study and modeling of methane adsorption and diffusion in shale. Fuel 117: 509-519.
9. Nuttall BC, Eble CF, Drahovzal JA, Bustin RM (2005) Analysis of Devonian black shales in Kentucky for potential carbon dioxide storage and enhanced natural gas production. Report Kentucky Geological Survey/University of Kentucky.
10. Nuttall BC (2010) Reassessment of CO2 storage capacity and enhanced gas recovery potential of middle and upper Devonian black shales in the Appalachian basin. In: MRCSP Phase II Topical Report. Kentucky Geological Survey Lexington Kentucky.
11. Fathi E, Akkutlu IY (2013) Multi-component Gas Transport and Adsorption Effects during CO2 Injection and Enhanced Shale Gas Recovery. Int J Coal Geol article in press.
12. Kalantari-Dahaghi A (2010) Numerical Simulation and Modeling of Enhanced Gas Recovery and CO2 Sequestration in Shale Gas Reservoirs. A feasibility study. Presented at the SPE International Conference on CO2 Capture Storage and Utilization New Orieans Louisiana SPE-139701-MS.
13. Kim TH, Cho J, Lee KS (2017) Evaluation of CO2 injection in shale gas reservoirs with multi-component transport and geomechanical effects. Appl Energy 190: 1195-1206.
14. Yu W, Al-shalabi EW, Sepehrnoori K (2014) A sensitivity study of potential CO2 injection for enhanced gas recovery in Barnett shale reservoirs. Presented at the SPE unconventional resources conference Woodlands Texas. SPE-169012-MS.
15. Liu J, Xie L, Yao Y, Gan Q, Zhao P et al. (2019) Preliminary Study of Influence Factors and Estimation Model of the Enhanced Gas Recovery Stimulated by Carbon Dioxide Utilization in Shale. ACS Sustainable Chem Eng 7: 20114-20125.
16. Sun H, Yao J, Gao S-H, Fan D-Y, Wang C-C, et al. (2013) Numerical Study of CO2 Enhanced Natural Gas Recovery and Sequestration in Shale Gas Reservoirs. Int J Greenhouse Gas Control 19: 406-419.
17. Martineau DF (2007) History of the Newark East Field and the Barnett Shale as a Gas Reservoir. AAPG Bull 91: 399-403.
18. Vermylen JP (2011) Geomechanical Studies of the Barnett Shale, Texas, USA. PhD Thesis Stanford University Palo Alto CA.
19. Younglove B, Ely JF (1987) Thermophysical Properties of Fluids: II. Methane, Ethane, Propane, Isobutane, and Normal Butane, American Chemical Society and the American Institute of Physics for the National Bureau of Standards.
20. Angus S, Armstrong B, Reuck KM (1976) International Thermodynamic Tables of the Fluid State-3 Carbon Dioxide. Pergamon, New York, Pergamon Press, Oxford.
21. Chang Y, Coats B, Nolen J (1996) A Compositional Model for CO2 Floods Including CO2 Solubility in Water. Paper SPE 35164 presented at the 1996 Permian Basin Oil and Gas Recovery Conference.
22. Duan Z, Mao S (2006) A thermodynamic model for calculating methane solubility, density and gas phase composition of methane-bearing aqueous fluids from 273 to 523K and from 1 to 2000 bar. Geochimica et Cosmochimica Acta 70: 3369-3386.
23. Oldenburg C, Pruess K, Benson SM (2001) Process modeling of CO2 injection into natural gas reservoirs for carbon sequestration and enhanced gas recovery. Energy & Fuels 15: 293-298.
24. Sing KSW, Everett DH, Haul RAW, Moscou L, Pierotti RA, et al. (1985) Reporting Physisorption Data for Gas/Solid Systems with Special Reference to the Determination of Surface Area and Porosity. Pure Appl Chem 57: 603-619.
25. Clarkson CR, Haghshenas B (2013) Modeling of Supercritical Fluid Adsorption on Organic-Rich Shales and Coal. Paper SPE 164532, SPE Unconventional Resources Conference, The Woodlands, TX.
26. Langmuir L (1918) The Adsorption of Gases on Plane Surfaces of Glass, Mica and Platinum. J Am Chem Soc 40: 1403-1461.
27. Gao C, Lee JW, Spivey JP, Semmelbeck ME (1994) Modeling Multilayer Gas Reservoirs Including Sorption Effects. Paper SPE 29173, SPE Eastern Regional Conference & Exhibition, Charleston, WV.
28. Freeman CM, Moridis GJ, Michael GE, Blasingame TA (2012) Measurement, Modeling, Diagnostics of flowing Gas Composition Changes in Shale Gas Wells. Paper SPE 153391, SPE Latin American and Caribbean Petroleum Engineering Conference Mexico.
29. Brunauer S, Emmett PH, Teller E (1938) Adsorption of Gases in Multimolecular Layers. J Am Chem So. 60: 309-319.
30. Arri LE, Yee D, Morgan WD, Jeansonne MW (1992) Modeling Coalbed Methane Production with Binary Gas Sorption. Paper SPE 24363, SPE Rocky Mountain Regional Meeting, Casper, WY.
31. Hall FE, Zhou C, Gasem Jr KAMRLR, Yee D (1994) Adsorption of Pure Methane, Nitrogen, and Carbon Dioxide and Their Binary Mixtures on wet Fruitland Coal. Paper SPE 29194, SPE Eastern Regional Meeting, Charleston, WV.
32. Anderson DM, Nobakht M, Moghadam S, Mattar L (2010) Analysis of Production Data from Fractured Shale Gas Wells. Presented at the SPE Unconventional Gas Conference, Pittsburgh, Pennsylvania SPE-131787-MS.
33. Yu W, Sepehrnoori K (2013) An Efficient Reservoir Simulation Approach to Design and Optimize Unconventional Gas Production. Paper SPE 165343, SPE Western Regional & AAPG Pacific Section Meeting, Monterey, CA.
34. Yu W, Sepehrnoori K (2013) Optimization of Multiple Hydraulically Fractured Horizontal Wells in Unconventional Gas Reservoirs. Paper SPE 164509, SPE Production and Operations Symposium, Oklahoma City, OK.
35. Yu W, Sepehrnoori K (2014) Simulation of Gas Desorption of Gas Desorption and Geomechanics Effects for Unconventional Gas Reservoirs. Fuel 116: 455-464.
36. Clark AJ, Lake LW, Patzek TW (2011) Production Forecasting with Logistic Growth Models. Paper SPE 144790 presented at the SPE Annual Technical Conference and Exhibition, Denver, CO, USA.
37. Tsoularis A, Wallace J (2001) Analysis of logistic growth models. Mathematical Biosciences 179: 21-55.